Aluminum K-Shell Line Emission as a Diagnostic in Light Ion Beam Fusion Experiments

J.J. MacFarlane, P. Wang,
T.A. Mehlhorn, J. Bailey, R.J. Dukart

March 1992

UWFDM-877

Presented at the 9th Topical Conference on High-Temperature Plasma Diagnostics, Santa Fe NM, 15–19 March 1992; Rev. of Sci. Instrum. 63 (1992) 5062.

FUSION TECHNOLOGY INSTITUTE

UNIVERSITY OF WISCONSIN

MADISON WISCONSIN

Aluminum K-Shell Line Emission as a Diagnostic in Light Ion Beam Fusion Experiments

J. J. MacFarlane and P. Wang

Fusion Technology Institute
Department of Nuclear Engineering and Engineering Physics
University of Wisconsin-Madison
Madison, Wisconsin, 53706

T. A. Mehlhorn, J. Bailey, and R. J. Dukart

Sandia National Laboratories
Albuquerque, New Mexico, 87185

March 1992

UWFDM-877

Presented at the 9th Topical Conference on High-Temperature Plasma Diagnostics, Santa Fe, NM, 15-19 March 1992. Submitted to Review of Scientific Instruments.

Abstract

K_α satellite line emission from targets irradiated by intense light ion beams can be used to diagnose plasma temperatures and densities. The fluorescence lines are created as 2p electrons drop down to fill 1s vacancies that result from ion beam-induced ionizations. We present results from collisional-radiative equilibrium calculations for thin Al diagnostic layers to illustrate the dependence of the K_α emission spectrum on temperature, density, and layer thickness. We also discuss the effects of opacity on the spectrum and the contribution from K_α transitions involving excited states.

1. Introduction

A number of recent experiments have demonstrated the value of using inner-shell x-ray spectroscopy in determining the physical properties of high temperature plasmas.[1–8] Absorption spectroscopy has been used in laser-heated target experiments to monitor plasma conditions,[4–7] measure opacities,[2] and determine the conditions in pusher regions during inertial confinement fusion (ICF) target implosions.[8] In absorption experiments, a second beam is used to heat a high-Z material to produce an x-ray backlighter source. In light ion beam fusion experiments, such as those performed at the Sandia National Laboratories PBFA-II and Kernforschungszentrum Karlsruhe KALIF facilities, emission spectroscopy can be used to diagnose plasma conditions.[1,9] In addition to heating the target, the beam also serves as a diagnostic probe by producing inner-shell vacancies in the target ions. As electrons drop down to fill the inner-shell vacancies, x-ray fluorescence lines are emitted. This negates the need for a backlighter x-ray source.

The first observation of K_α satellite emission spectra in an intense proton beam experiment on PBFA-II was recently reported by Bailey et al.[1] In this experiment an Al conical target was irradiated by a 4-6 MeV proton beam with a pulse width of 15-20 ns and a power density of approximately 1-2 TW/cm^2. The proton beam produces 1s vacancies, which are quickly filled by spontaneous transitions from the 2p shell. Because of reduced electron screening effects, the K_α lines for ions from Al IV (Ne-like) to Al XII (He-like) tend to exhibit small, but detectable shifts to shorter wavelengths. Observing the K_α satellite spectrum therefore provides information about the ionization distribution of the target plasma, and from that constraints on the plasma conditions.

In this paper, we present results from collisional-radiative equilibrium (CRE) calculations which illustrate the sensitivity of the K_α spectrum to plasma conditions. A more detailed description of the physical processes which affect K_α spectra and our comparison with experimental results is presented elsewhere.[10] Emission and absorption

spectra are shown for a range of temperatures and densities that are typical of those currently attained in light ion beam fusion experiments. In addition, we show that the contribution of excited states to K_α emission spectra can be significant. We also discuss the dependence of the total flux emitted in the K_α spectral region on the thickness of the Al target. This type of information can be used as a guide to determine the optimum thickness of diagnostic tracers in experiments.

2. Theoretical Models

Spectral properties are computed using a CRE code which solves multilevel statistical equilibrium equations self-consistently with the ion beam properties and radiation field.[10−13] For the plasma conditions discussed in this paper, the distribution of atomic level populations should be fairly close to local thermodynamic equilibrium — the exception to this being of course the autoionizing levels populated by the ion beam. We have therefore neglected photoexcitation and photoionization effects. Atomic level populations are determined using a detailed configuration accounting (DCA) model in which the following processes are considered: collisional excitation, deexcitation, ionization, and recombination; spontaneous decay, radiative and dielectronic recombination; and proton-impact ionization and autoionization. Except for dielectronic recombination, every state of an ionization stage is coupled to every other state of that ion and each state of the next higher ionization state. Only the ground states of adjacent ions are coupled by dielectronic recombination. A summary of our models for computing rate coefficients is described elsewhere.[11,14] To compute spectral properties we consider emission and absorption from bound-bound, bound-free, and free-free transitions, as well as inner-shell bound-free attenuation. Voigt line profiles are used which include the effects of natural, Doppler and Stark broadening.

Our atomic model for Al consists of 750 levels distributed over all 14 ionization stages. Of these roughly half are autoionizing levels which account for a total of

about 600 K_α transitions. Level energies and oscillator strengths were computed using a single-configuration Hartree-Fock model[15] with relativistic corrections. L-S coupling is used to approximate the interaction between bound electrons. Proton-impact ionization cross sections were computed using a plane-wave Born approximation model.[16] Fluorescence yields were taken from calculations by E. McGuire as tabulated in Ref. 17. A detailed description of our atomic physics calculations for K_α transitions will be presented elsewhere.[18]

3. Results

Emission and absorption properties were computed for idealized plane-parallel plasmas with uniform temperatures and densities. The thickness of the diagnostic layers corresponds to 10 Å – 100 μm Al foils at solid density. The greatest thickness is roughly equivalent to the stopping range of 5 MeV protons in Al. The purpose of using a much thinner layer of Al would be to serve as a diagnostic tracer, as opposed to stopping the beam. In each calculation the beam is assumed to be uniform and monoenergetic, with 5 MeV protons at a power density of 5 TW/cm^2.

In our first set of calculations, we examine the contribution of excited states to the K_α emission spectrum. That this effect might be important in ion beam experiments was suggested by R. Mancini.[19] Their importance has also recently been demonstrated in absorption experiments.[2,3] Figure 1 shows the results from two calculations which were identical except for the following. The spectrum indicated by the lighter shading was computed using only those autoionizing levels which are produced from proton-impact ionization of an ion in its ground state configuration. The spectrum represented by the darker shading represents results in which autoionizing levels produced from both ground state and excited state configurations up to $n = 3$ are considered. In each case the plasma temperature was $T = 25$ eV, the ion density was $n = 10^{-1}\, n_0$ ($n_0 \equiv$ solid density), and

the plasma thickness was $L = 1\,\mu$m (i.e., the original foil thickness prior to expansion was $L_0 = 0.1\,\mu$m). At this temperature, K_α lines from Al IV-VI dominate the spectrum.

The most noticeable contribution from excited states to the emission spectrum at this temperature is the rather broad features underlying the relatively narrow features of the low-lying states. As an illustration, the narrow features in the 1495 eV – 1505 eV range are produced primarily by transitions whose original states are in the ground state configuration of Al V:

$$1s^2 2s^2 2p^5 \xrightarrow[\text{p-impact}]{} 1s^1 2s^2 2p^5 \xrightarrow[K_\alpha]{} 1s^2 2s^2 2p^4.$$

The broad features are produced by Al IV transitions of the type:

$$1s^2 2s^2 2p^5 3l \xrightarrow[\text{p-impact}]{} 1s^1 2s^2 2p^5 3l \xrightarrow[K_\alpha]{} 1s^2 2s^2 2p^4 3l$$

where l represents an s, p, or d subshell. These lines are considerably broadened[20] because the lifetime for electrons excited to the n = 3 shell is considerably shorter than if they were to reside in the n = 2 shell. The wavelengths for the excited state Al IV transitions are similar to the ground state Al V transitions because the $n = 3$ electron has little effect on the interior electronic structure seen by electrons transiting from the 2p to 1s shell.

Figure 2 shows the dependence of the K_α spectrum on temperature. In each case $n = 10^{-2}\,n_0$ and $L = 1\,\mu$m ($L_0 = 100$ Å). At 30 eV, the most prominent spectral features are those from Al VI. (The features are labeled by the ions which contribute most prominently, though not exclusively, to that spectral region.) At $T = 60$ eV, transitions from Al X and Al XI dominate.

Figure 3 shows the attenuation factor ($\equiv e^{-\kappa_\nu L}$, where κ_ν is the absorption coefficient and L is the plasma width) for the same set of calculations. The results indicate that for an Al diagnostic tracer with an original thickness of 100 Å, the line center op-

tical depths of the most prominent lines are of order unity. This suggests that even for extremely thin tracers line self-attenuation will affect the observed spectrum.

Figure 4 illustrates how the emission spectrum changes as the density is varied. In each calculation, we computed the spectrum for an Al tracer foil with an original thickness of $L_0 = 100$ Å that was heated to $T = 60$ eV. The top spectrum corresponds to a foil that expanded 10 times ($n = 10^{-1}\, n_0$, $L = 10\, L_0$) while the bottom spectrum corresponds to a foil that expanded 100 times. The most noticeable impact is the shift to lower ionization stage as the density increases. In addition, individual lines are seen to broaden in the high density case, and the relative intensity of lines is affected.

Finally, we have computed the absolute K_α flux integrated from 1480 eV to 1620 eV for Al foil thicknesses ranging from 10 Å to 100 μm. The purpose of these calculations is to show how the flux falls off as the foil thickness decreases, and thereby give some guidance to experimentalists who must study the trade-offs between detector sensitivity, opacity effects, ion stopping effects, and so forth. Figure 5 shows how the calculated flux varies with foil thickness for a plasma at $T = 60$ eV and $n = 10^{-2}\, n_0$. Note that for very thin foils the flux decreases roughly linearly with thickness because opacity effects are relatively unimportant. However, the flux for foils with thickness $\gtrsim 10\,\mu$m becomes constant. This is because the plasma becomes optically thick at all wavelengths in this spectral region due to L-shell photoabsorption.

4. Summary

Results from CRE calculations have been presented which show how K_α satellite line emission can be used to deduce plasma properties in intense ion beam experiments. We have described the sensitivity of K_α emission spectra to the temperature, density, and thickness of a thin Al diagnostic layer. It has also been shown that K_α transitions involving excited states of moderately ionized Al can make a significant contribution to

the spectrum. These calculations suggest that inner-shell x-ray spectroscopy can be a valuable diagnostic tool for determining plasma conditions in light ion beam fusion.

5. Acknowledgements

This work was supported by Sandia National Laboratories and Kernforschungszentrum Karlsruhe. Computing support has been provided in part by the National Science Foundation through the San Diego Supercomputing Center.

6. References

1. J. Bailey, A. L. Carlson, G. Chandler, M. S. Derzon, R. J. Dukart, B. A. Hammel, D. J. Johnson, T. R. Lockner, J. Maenchen, E. J. McGuire, T. A. Mehlhorn, W. E. Nelson, L. E. Ruggles, W. A. Stygar, and D. F. Wenger, Lasers and Particle Beams **8**, 555 (1990).

2. T. S. Perry, S. J. Davidson, F. J. D. Serduke, D. R. Bach, C. C. Smith, J. M. Foster, R. J. Doyas, R. A. Ward, C. A. Iglesias, F. J. Rogers, J. Abdallah, Jr., R. E. Stewart, J. D. Kilkenny, and R. W. Lee, Phys. Rev. Lett. **67**, 3784 (1991).

3. J. Abdallah, Jr., R. E. H. Clark, and J. M. Peek, Phys. Rev. **A 44**, 4072 (1991).

4. C. Chenais-Popovics, C. Fievet, J. P. Geindre, J. C. Gauthier, E. Luc-Koenig, J. F. Wyart, H. Pepin, and M. Chaker, Phys. Rev. **A 40**, 3194 (1989).

5. J. Bruneau, C. Chenais-Popovics, D. Desenne, J.-C. Gauthier, J.-P. Geindre, M. Klapisch, J.-P. Le Breton, M. Louis-Jacquet, D. Naccache, and J.-P. Perrine, Phys. Rev. Lett. **65**, 1435 (1990).

6. S. J. Davidson, J. M. Foster, C. C. Smith, K. A. Warburton, and S. J. Rose, Appl. Phys. Lett. **52**, 847 (1988).

7. D. M. O'Neil, C. L. S. Lewis, D. Neely, and S. J. Davidson, Phys. Rev. **A 44**, 2641 (1991).

8. A. Hauer, R. D. Cowan, B. Yaakobi, O. Barnouin, and R. Epstein, Phys. Rev. **A 34**, 411 (1986).

9. E. Nardi, and Z. Zinamon, J. Appl. Phys. **52**, 7075 (1981).

10. J. J. MacFarlane, P. Wang, J. Bailey, T. A. Mehlhorn, R. H. Dukart, and R. Mancini, in preparation (1992).

11. J. J. MacFarlane, and P. Wang, Lasers and Particle Beams, in press (1992).

12. J. J. MacFarlane, and P. Wang, Lasers and Particle Beams **8**, 729 (1990).

13. J. J. MacFarlane, P. Wang, and D. L. Henderson, University of Wisconsin Fusion Technology Institute Report UWFDM-873, Madison, WI (1992).

14. P. Wang, Ph.D. Dissertation, Department of Nuclear Engineering and Engineering Physics, University of Wisconsin, Madison, WI (1991).

15. C. F. Fischer, *The Hartree-Fock Method for Atoms* (Wiley, New York, 1977).

16. D. H. Madison, and E. Merzbacher, in *Atomic Inner-Shell Processes*, edited by B. Crasemann (Academic, New York, 1975).

17. D. Duston, R. W. Clark, J. Davis, and J. P. Apruzese, Phys. Rev. **A 27**, 1441 (1983).

18. P. Wang, J. J. MacFarlane, and G. A. Moses, in preparation (1992).

19. R. Mancini, personal communication (1991).

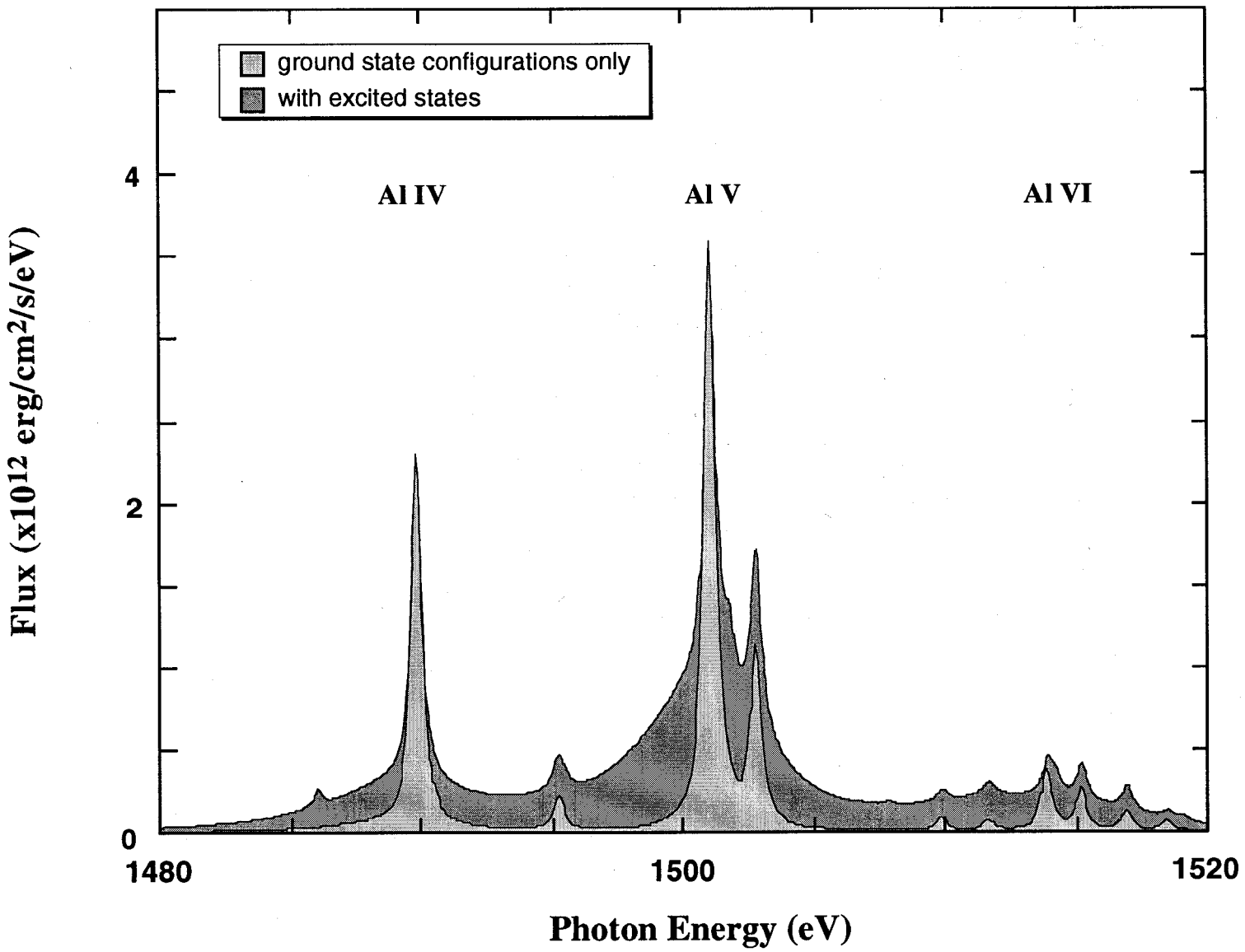

Figure 1. Calculated K_α emission spectrum for an Al plasma at $T = 25$ eV, $n = 10^{-1}\, n_0$, and $L = 1\ \mu$m. The contribution from excited state configurations is indicated by the darker shaded region.

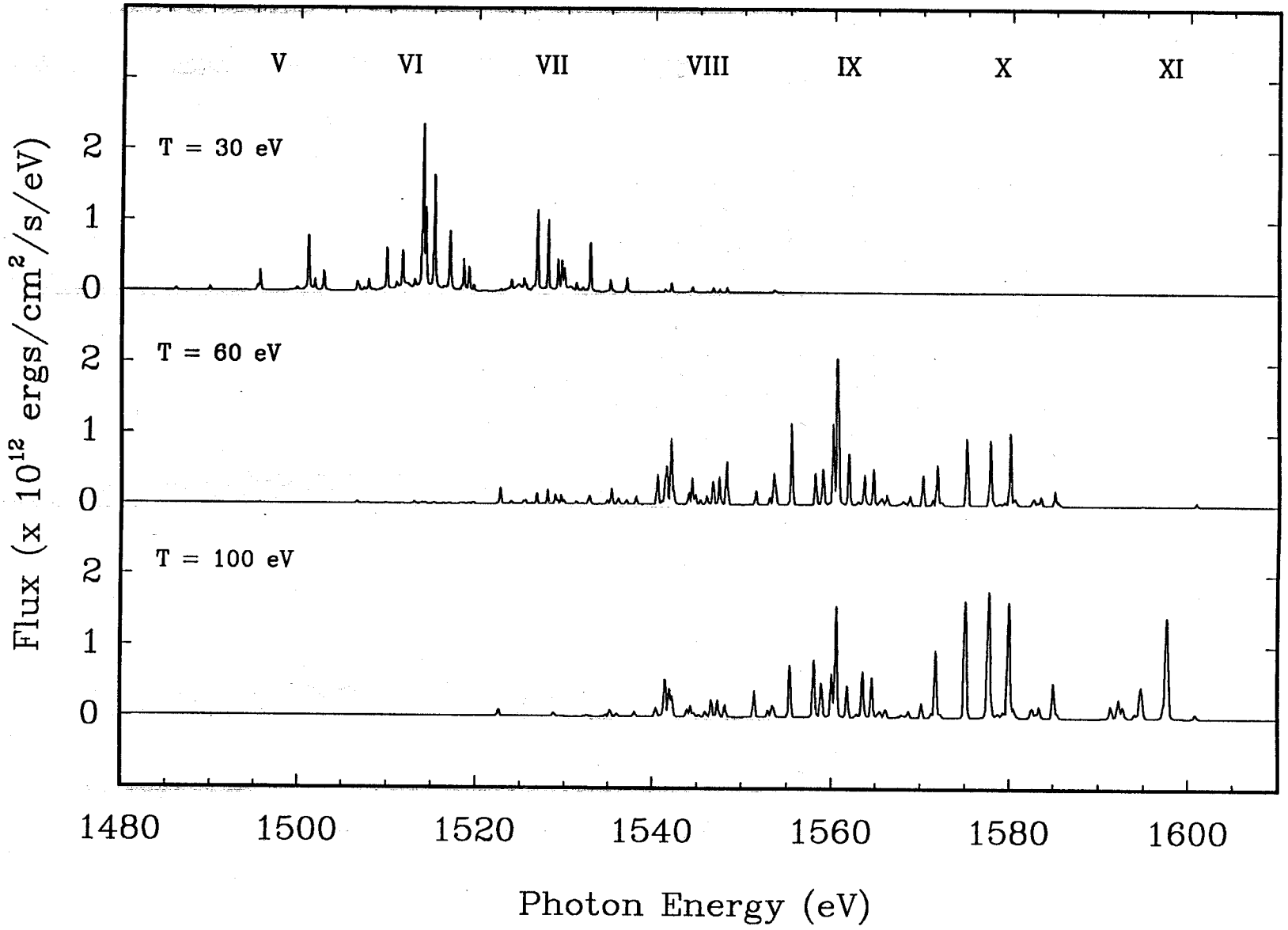

Figure 2. K_α emission spectra calculated for Al plasmas at $T = 30, 60$, and 100 eV. In each case $n = 10^{-2}\, n_0$ and $L = 1$ μm.

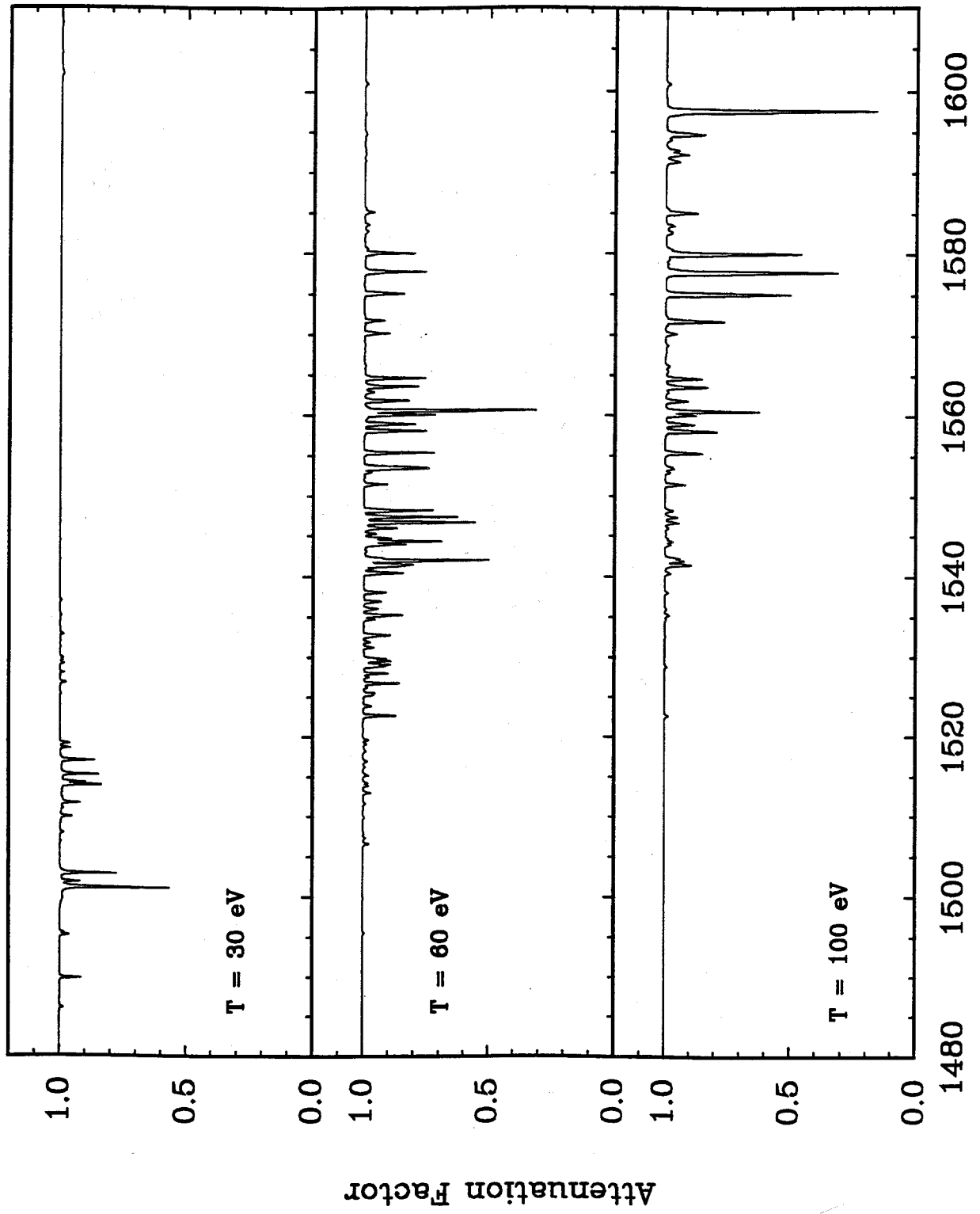

Figure 3. Attenuation factor for Al diagnostic layers as a function of temperature. Plasma conditions are the same as those indicated in Figure 2.

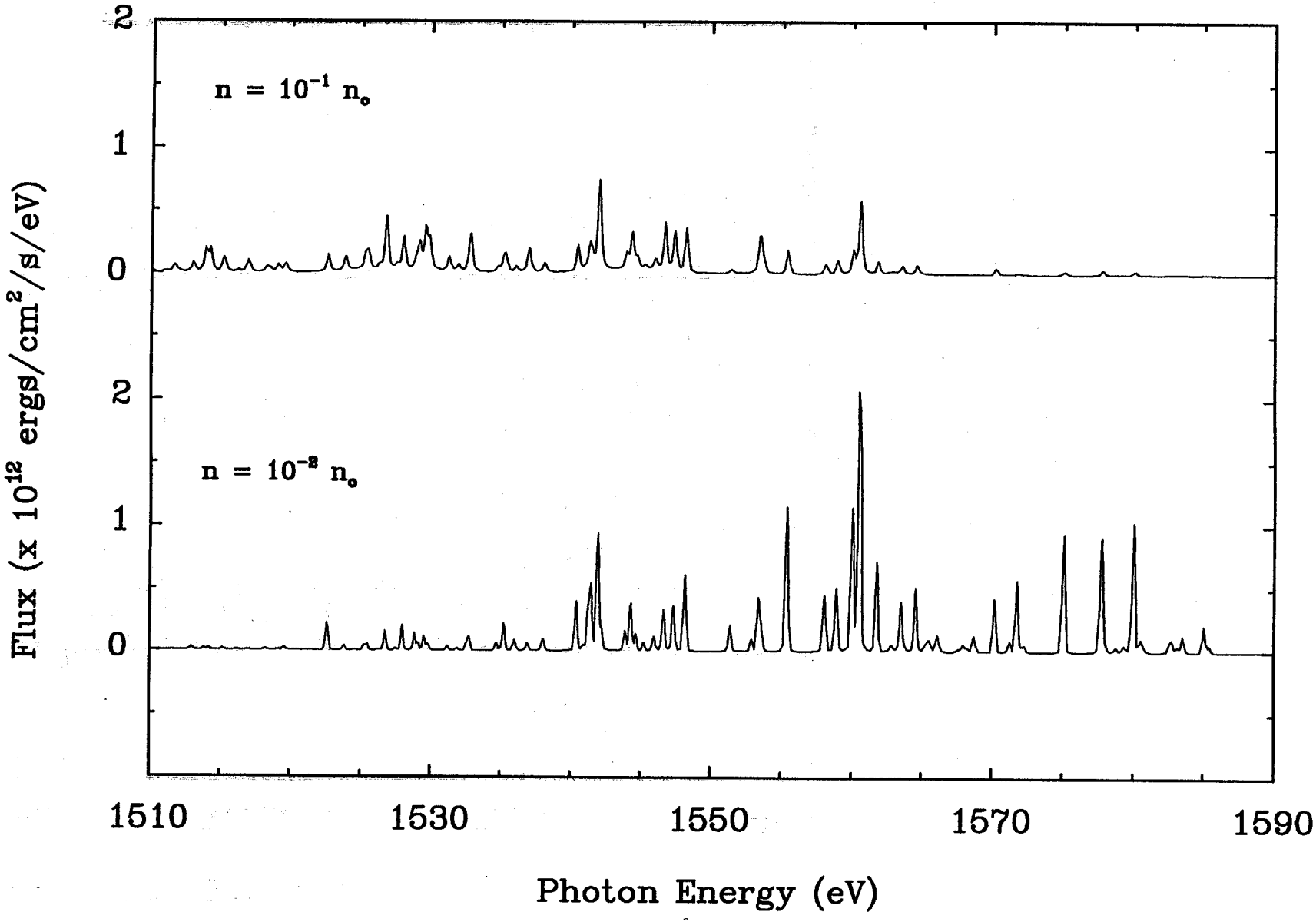

Figure 4. K_α emission spectra calculated for 100 Å Al foils which have expanded 10 times (top) and 100 times (bottom). In each case $T = 60$ eV.

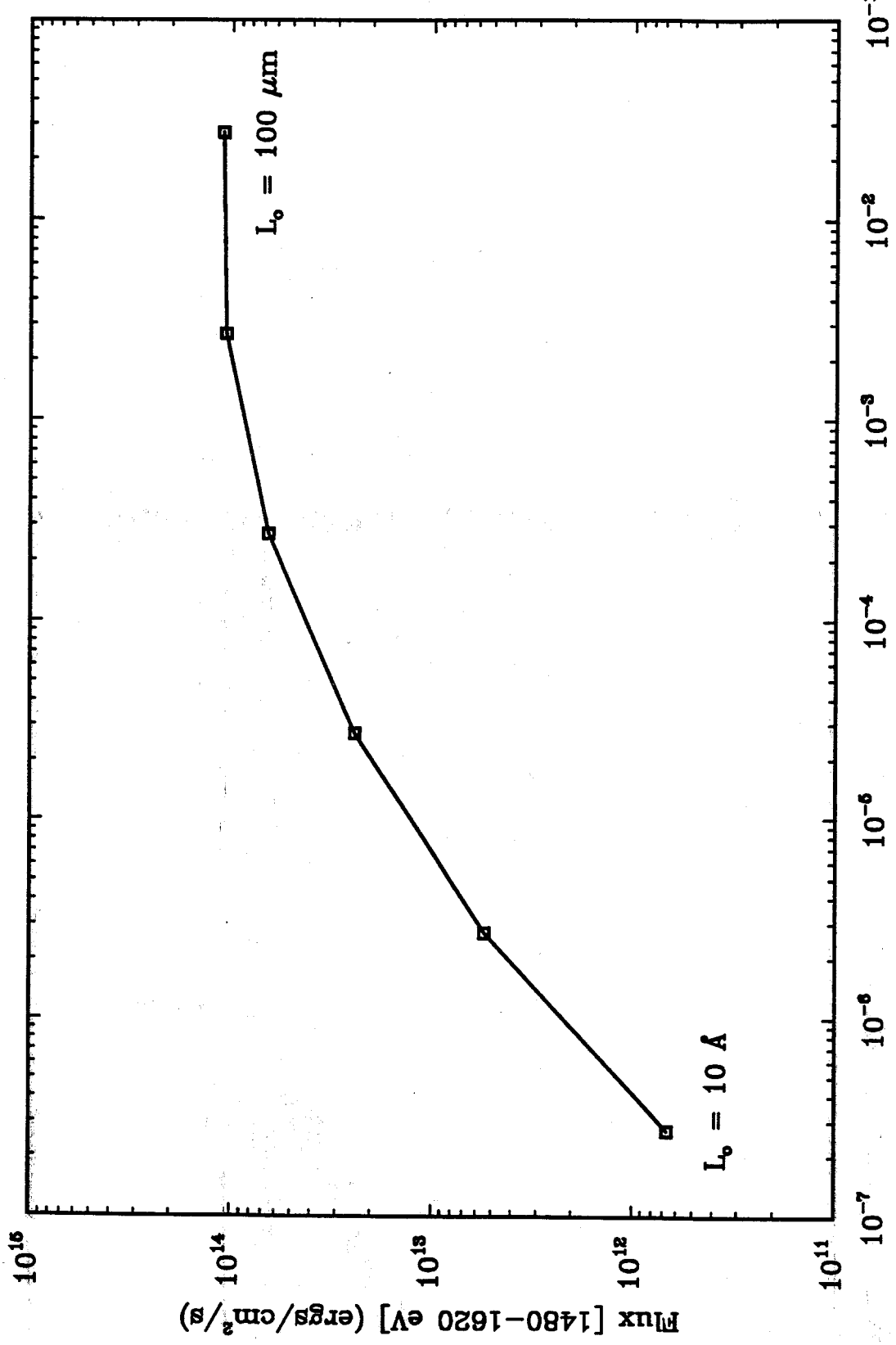

Figure 5. Dependence of frequency-integrated flux in the spectral region from 1480 eV to 1620 eV on Al foil thickness. In each case $T = 60$ eV and $n = 10^{-2}\, n_0$.